Estimate of Red-Cell Deformability and Plasma Viscosity Based on Flow Curve

S. Ookawara, A. Yano, and K. Ogawa
Dept. of Chemical Engineering, Tokyo Institute of Technology, Tokyo 152-8552, Japan

K. Taniguchi
Dept. of Cardiology, Gunma Prefectural Cardiovascular Center, Maebashi, Gunma 371-0004, Japan

A new estimation method of clinical blood indices based on the flow characteristics of unadjusted whole blood is proposed, such as red-cell deformability and plasma viscosity. Parameter values of Bingham and power law models were calculated based on the measured flow characteristics. Red-cell deformability was measured by the method of laser diffractometry. The clinical indices were related with the non-Newtonian model parameters by a feedforward neural network (NN). Inputs of the NN are the parameter values and hematocrit. Outputs are red-cell deformability and plasma viscosity. It was verified that estimated values agreed well with those measured values after sufficient learning. By applying this method to 20 healthy persons, it was confirmed that the estimated values by NN were within normal range. According to these experimental results, this estimation method can be applied to clinical use.

Introduction

It is well known that the physical and biochemical properties of whole blood and its composition vary with health condition. Therefore, these properties have been treated as clinical indices. Whole blood is roughly divided into two components, red cells and plasma, whose volume fractions are usually around 0.4 and 0.6, respectively. Although under no stress, red-cell shape is like that of a flat and biconcave disk, its shape is considerably changed by small amounts of stress, thus allowing it to flow in a capillary whose inner diameter is smaller than that of the red cell. This ability is called *deformability*. It should be noted that this ability contributes to the achievement of the incredibly low viscosity of whole blood in spite of its high concentration.

It is reported that red-cell deformability is decreased in connection with some diseases such as sickle cell disease (Green et al., 1988; Clark et al., 1980; Evans et al., 1984; Keidan et al., 1989; Schmalzer et al., 1989), hereditary spherocytosis (Ikemoto et al., 1998; Nagasawa, 1992), iron deficiency anemia (Yip et al., 1983; Ikemoto et al., 1989), diabetes (Maeda et al., 1990), and so on. Therefore, there is a large amount of literature on its measuring techniques, such as the micropipette technique (Evans and La Celle, 1975), filtration (Usami et al., 1975), rheoscope (Schmid-Schönbein and Wells, 1969), centrifugal elongation (Nagasawa, 1981), laser diffractometry (Bessis and Mohandas, 1975), and so on. All this attention is clearly because red-cell deformability is a very important clinical index. Plasma viscosity is also considered an important clinical index, since it plays an especially important role in microcirculation.

To our knowledge, however, there is no practically established measurement technique for both indices, which meets such clinical demands as easy handling and quick measurement, since the procedures are usually rather tedious. For instance, the separation of red cells and plasma by a centrifuge and the wash of red cells with a physiological saline are very time-consuming steps as performed in this study for the preparation of test fluids.

Since the two main components of blood are red cells and plasma, as just mentioned, it is reasonable to assume that the flow characteristics of whole blood are determined mostly by hematocrit (volume fraction of red cells Hct) and its aforementioned properties, namely, red-cell deformability and plasma viscosity. If the relation is elucidated, therefore, there is a possibility that those indices could be predicted from the

Correspondence concerning this article should be addressed to S. Ookawara.

flow characteristics of whole blood. Actually, Chien (1978) suggested that the measurement of red-cell suspension viscosity is useful as an indirect measurement of cell deformability. In his study, however, it is strongly recommended that the hematocrit should be adjusted to a constant level and that red-cell deformability tests should be performed on suspensions of red cells in a buffered Ringer's solution (pH 7.4) rather than the whole blood, to avoid the changes of other parameters. The tedious procedures associated with his method have therefore undoubtedly prevented its practical clinical use. From a clinical viewpoint, the authors argue that it is preferable to estimate the red-cell deformability from the flow characteristics of unadjusted fresh whole blood rather than from the recommended suspension.

At present the relation between the flow characteristics of whole blood and such factors as the hematocrit, the deformability of red cells, and plasma viscosity has not been clear enough. However, the causes are probably because the experiments are time-consuming, that there is no way to express the relation, and that there is no correlation method for the expected complicate relation.

In this study, we prepared proper blood samples, and the hematocrit, red-cell deformability, and plasma viscosity are artificially adjusted to elucidate the relation experimentally. The flow characteristics of these prepared blood samples were measured by using a capillary-type viscometer that we had developed in our previous works (Ogawa et al., 1991; Ogawa et al., 1994). Its superior features as a clinical viscometer, which meets the clinical demands just mentioned, strongly support the realization of the method proposed in this study. We applied Bingham and power law models for extraction and to quantify the features of the measured flow characteristics. By drawing contour maps of these non-Newtonian parameters on plasma viscosity-deformability index plane, we investigated the relation and the possibility of prediction. Based on the results obtained from comprehensive experiments, we correlated these indices with the flow characteristics, by using a feedforward artificial neural network that was proven to approximate any function with a finite number of discontinuities with arbitrary accuracy (Demath and Beale, 1994). The feasibility of this method was tested by applying it to 20 healthy donors.

Experiments and Results

Preparation of blood samples

Blood samples were collected from two donors who were healthy adult males. After collection, these blood samples were properly treated with anticoagulant and immediately packed into the blood transfusion bags. A preservative solution of citrate-phosphate-dextrose (CPD) was used as an anticoagulant in this study; it contains 2.630 g of sodium citrate, 0.327 g of citric acid, 2.320 g of glucose, and 0.251 g of sodium dihydrogenphosphate dihydrate per 100 mL. Fifty-six mL of the preservative was added to 400 mL of fresh whole blood. These blood samples were separated into blood cells and plasma by a centrifuge (1,500 g, 10 min). The plasma viscosity μ_p was decreased by diluting with a physiological saline and increased by adding the proper amount of dextran (molecular weight = 40,000). The adjusted plasma viscosity values were approximately 0.9, 1.2, 1.5, 1.8×10^{-3} Pa·s. On the other hand, the separated red cells were washed with a physiological saline three times and they were heat-treated for 10 min in bath maintained at 48°C and 49°C (Nagasawa, 1992) to obtain three types of red cell samples: two different levels of decreased deformability and normal. By blending one of three red-cell samples and one of four plasma samples, we prepared blood samples with adjusted levels of hematocrit of ap-

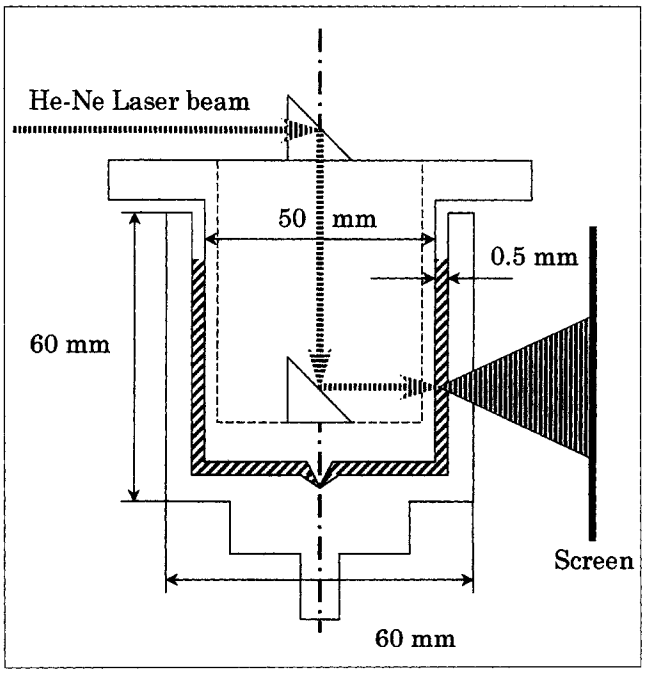

Figure 1. Apparatus for the laser diffraction method.

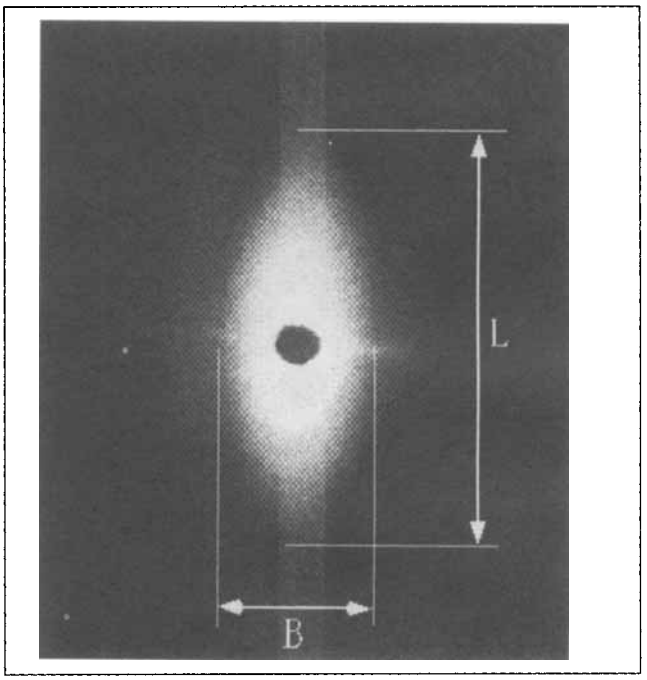

Figure 2. Minor axis length *B* and major axis length *L* of diffraction image measured in this study for the calculation of the DI.

proximately 27, 37, 47 and 57. Finally, we obtained 48 samples that combine all of them.

Measurements of red-cell deformability

In this study, the laser diffraction method (Bessis and Mohandas, 1975) was used to measure the deformability of red cells. Figure 1 shows the apparatus, which consists of coaxial cylinders and a He–Ne laser. The gap between the two cylinders is 0.5 mm, and it is filled with dilute red-cell suspension. The medium is 20 wt. % of the dextran phosphate buffered saline (PBS) solution whose viscosity is about 0.020 Pa·s at ambient condition. The inner cylinder is fixed and the outer one is rotated at a given speed by a motor so that red cells are exposed to adjusted shear stress, τ. By means of two prisms set inside the inner cylinder, the diffraction image of red cells is obtained on the screen, which is recorded on videotape. The interaction between red cells in a test fluid is expected to be negligible, since the hematocrit of all samples is adjusted to 8×10^{-4}.

In this study, the minor axis length B and major axis length L of the diffraction image recorded on videotape were measured on a personal computer, as shown in Figure 2. Subse-

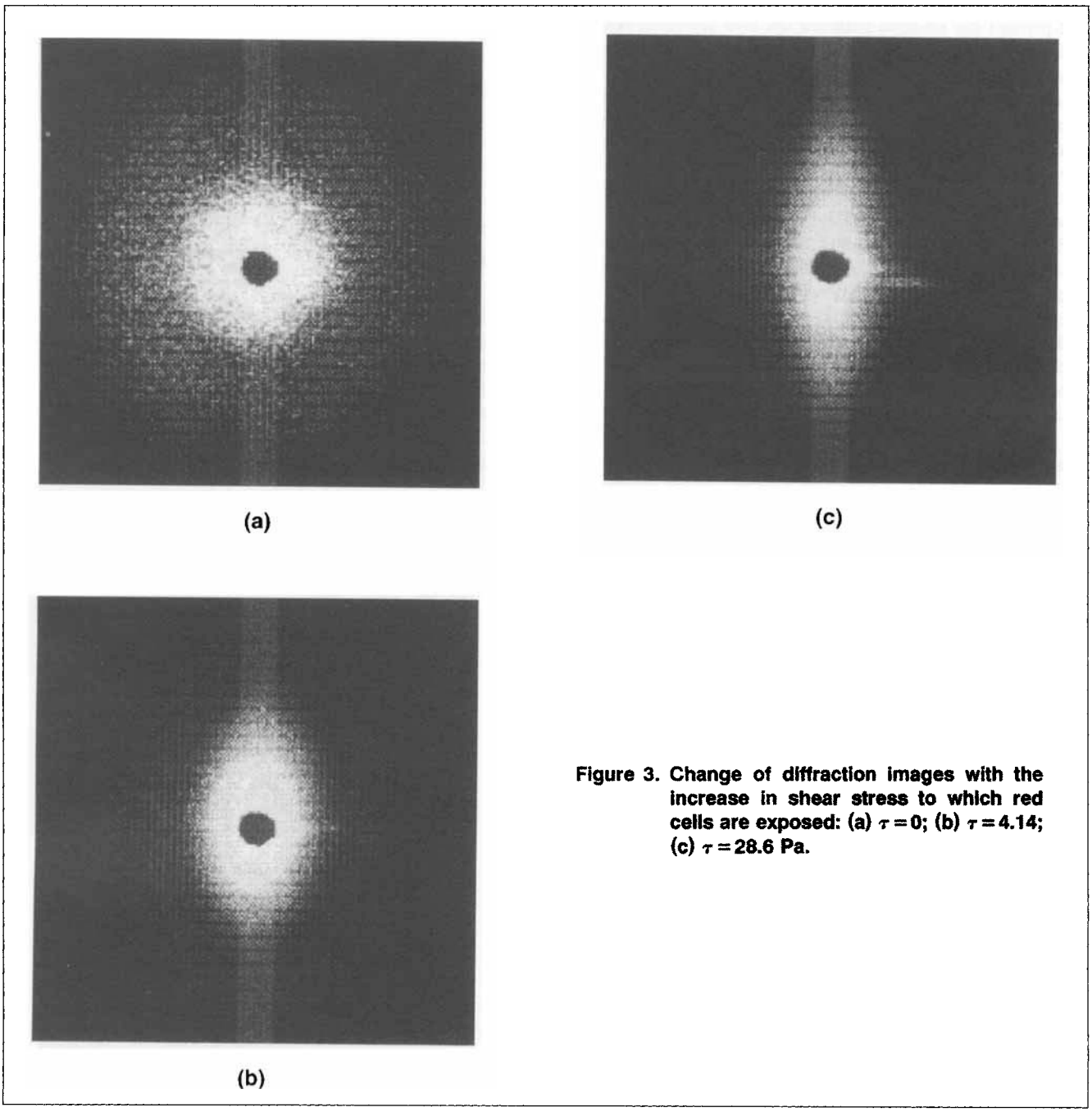

Figure 3. Change of diffraction images with the increase in shear stress to which red cells are exposed: (a) $\tau=0$; (b) $\tau=4.14$; (c) $\tau=28.6$ Pa.

quently, a deformation index (DI) was calculated from these values to evaluate the deformability of red cells based on the following equation:

$$\mathrm{DI} = \frac{L - B}{L + B}. \tag{1}$$

The DI value reflects the degree of cell elongation caused by a given shear stress, and it increases with the degree of deformation in the red cells in the suspension. The deformability of red cells is often evaluated by this value in the literature.

Figure 3 shows the obtained diffraction images of red cells on the screen. Under no shear stress, a circular image is obtained, as shown in Figure 3a. The shapes of these images change from circular to oval with increasing shear stress, as shown in Figures 3b and 3c. These changes are caused by elongation of the red cells. Figure 4 shows the relation between the shear stress and DI of each red-cell sample. In this figure, curve (A) shows the DI of a normal red cell, while curves (B) and (C) show the DI of heat-treated red cells at 48°C and 49°C, respectively. It can be seen that the deformability of heat-treated red cells is apparently decreased with the treatment temperature compared with the normal deformability. Ikemoto et al. (1998) and Nagasawa (1992) examined the red-cell deformability of hereditary spherocytosis, and reported that the DI measured by laser diffraction methods varies around 0.05 to 0.3 and 0.16 to 0.43 in the shear-stress range of 7.7 to 68 and 4 to 22 Pa, respectively. Therefore, it can be said that the experimental conditions of this study sufficiently covered the clinical range, though it is thought that different factors result in the same range of decreased deformability in the cases of heat treatment (Ham et al., 1968) and heredity spherocytosis (Mohandas and Chasis, 1993).

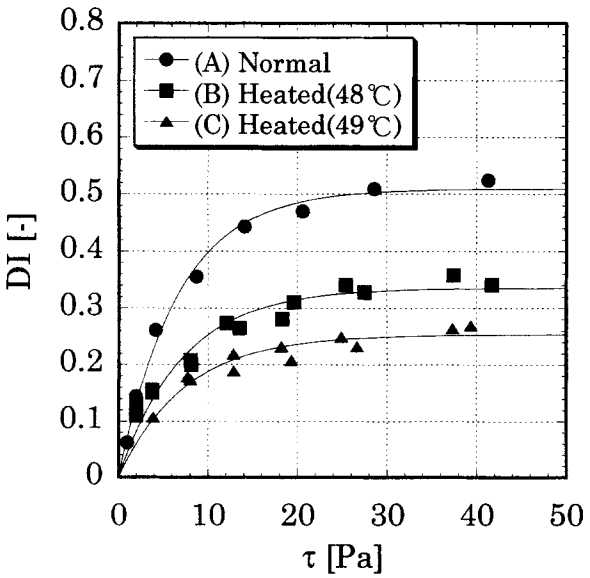

Figure 4. DI change with shear stress to which red cells are exposed.

Measurements of flow curve of whole blood and plasma viscosity

The flow characteristics of whole blood were measured in the shear rate range of 100 to 10,000 s^{-1} by the clinical blood viscometer developed in our previous works (Ogawa et al., 1991, 1994). Since plasma is usually known as Newtonian fluid, only viscosity was measured by the viscometer (Ogawa et al., 1991). Figure 5 shows typical relations between the shear rates $\dot{\gamma}$ and apparent viscosity μ_a of the blood samples. It can be seen in these figures that the individual dependency of flow characteristics on the deformability, plasma viscosity, and hematcrit are apparently different. If the deformability and plasma viscosity are normal and constant, the rise of apparent viscosity with the increase of hematocrit can be seen over the entire shear rate range (Figure 5a), and especially in the lower shear rate range. On the other hand, in the case where the hematocrit and the deformability are fixed as normal, the flow curves appear to show upward parallel translation with the increase in plasma viscosity (Figure 5b). When only the deformability is decreased with constant hematocrit and plasma viscosity, which are in the normal range, the apparent viscosity increases in the lower shear rate range, though not in the higher shear rate range. Consequently, the flow curves appear to rotate clockwise around the axis that seems to exist in the highest shear rate range with the decrease in the deformability (Figure 5c).

Analysis of Flow Curve

Adopted non-Newtonian models for the analysis

Clinical indices such as red-cell deformability and plasma viscosity μ_p have been considered to be useful but practically difficult to be measured because of the tedious measurement procedures. The flow curve of whole blood in the shear rate range of 100 to 10,000 s^{-1}, however, can be easily measured without hemolysis by the viscometer developed in the works of Ogawa et al. (1991, 1994), as shown in Figure 5. Therefore, it is extremely useful from a clinical viewpoint to estimate red-cell deformability and μ_p based on the flow characteristics in the shear rate range discussed earlier. However, if the Newtonian model is applied to describe the measured flow curve and the Newtonian viscosity μ_N of a blood sample is related to red-cell deformability and μ_p with constant hematocrit, it is impossible to predict red-cell deformability and μ_p from μ_N, since a different combination of red-cell deformability and μ_p could result in the same value of μ_N. Therefore, Bingham and power law models (Eqs. 2 and 3) were adopted as non-Newtonian models to describe the flow characteristics of all prepared blood samples in the shear rate range of 100 to 100,000 s^{-1}, which were measured in this study. The least-squares method was utilized to determine the four parameter values, Bingham viscosity μ_B, yield stress τ_y, fluid consistency k, and behavior index n:

$$\tau = \mu_B \dot{\gamma} + \tau_y \tag{2}$$

$$\tau = k\dot{\gamma}^n, \qquad (3)$$

where τ and $\dot{\gamma}$ are shear stress and shear rate, respectively.

The authors expect that the values of those four parameters and those combinations could contain the necessary amount of information to predict the values of those factors that decide the flow characteristics, namely, red-cell deformability and plasma viscosity. The reason two models are needed is discussed later.

Contour map of flow curve parameters

In this study, the contour maps of the four parameter values of prepared blood samples are drawn based on the experimental data calculated as described before. Figure 6 shows the typical dependency of each parameter value on the red-cell deformability and plasma viscosity μ_p with a constant hematocrit of 47. In this study, the deformability was evaluated by the DI value at the shear stress of 30 Pa, DI_{30}. In these figures, horizontal and vertical axes represent the

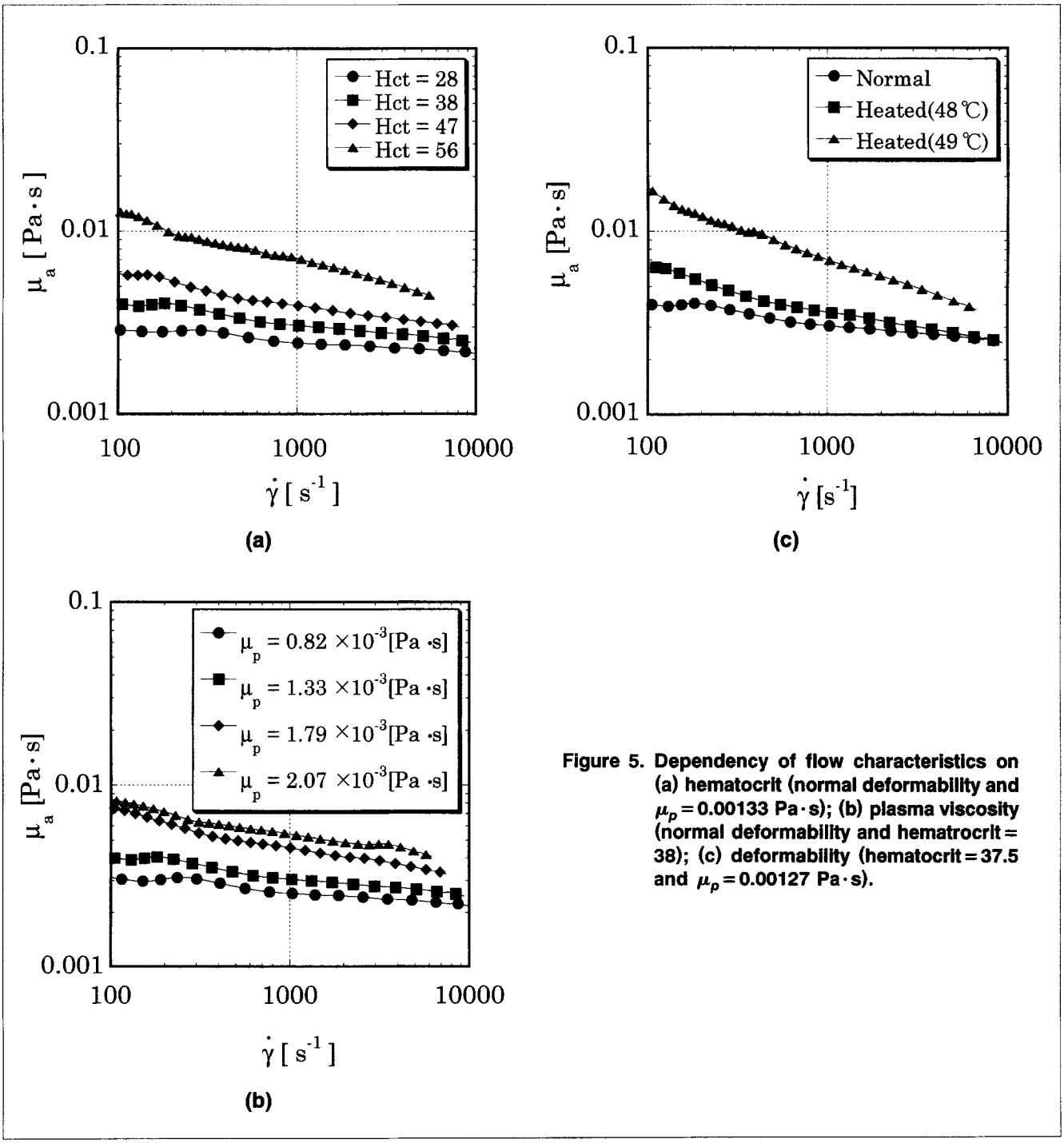

Figure 5. Dependency of flow characteristics on (a) hematocrit (normal deformability and $\mu_p = 0.00133$ Pa·s); (b) plasma viscosity (normal deformability and hematrocrit = 38); (c) deformability (hematocrit = 37.5 and $\mu_p = 0.00127$ Pa·s).

Table 1. Measured Parameter Values for Normalization

Parameter	X_{max}	X_{min}
μ_B [Pa·s]	0.00753	0.00173
τ_y [Pa]	4.12	0.12
n	0.97	0.56
Hct	57	27
μ_p [Pa·s]	0.0018	0.0009
DI_{30}	0.51	0.25

plasma viscosity, and the defined deformability DI_{30}. From these figures, it can be seen that Bingham viscosity mainly depends on plasma viscosity, but also on DI_{30} in the smaller DI_{30} range. This tendency was consistent at any hematocrit level. While three of the values—yield stress τ_y, index n, and consistency k—strongly depend on DI_{30}, and the dependencies of these three parameter values differ slightly from each other at hematocrit 47. Figure 7 shows that the contour maps of n vary with the hematocrit. The pattern seems to rotate clockwise. It is verified that contour maps of three parameter values—τ_y, n, and k—show a similar rotation of the pattern with hematocrit. From these figures, it can be seen that each parameter value shows a different dependency on the plasma viscosity and DI_{30} under the constant hematocrit, and that the dependencies are relatively monotonous. Therefore, a combination of measured flow-characteristics parameter values gives a unique set of plasma viscosity and DI_{30} values under the assumption that the hematocrit is known. This finding confirms the possibility of a quantitative prediction of DI_{30} and μ_p from the flow characteristics and hematocrit.

Prediction of Deformability and Plasma Viscosity

Artificial neural network

In this study, a feedforward artificial neural network, shown in Figure 8, was utilized for the correlation of the flow characteristics with the clinical indices such as red-cell deformability and plasma viscosity. The artificial neural network, which has sigmoid functions in a hidden layer and linear functions in the next output layer, has been proved to be capable of approximating any function with a finite number of discontinuities with arbitrary accuracy (Demath and Beale, 1994).

Based on the preceding discussion, the Bingham viscosity μ_B, yield stress τ_y, behavior index n, and hematocrit are selected as inputs of the network. Since the measurement of the hematocrit is a routine procedure for blood tests and very easy in a hospital, it is possible that the value is used as an input of the network from the clinical viewpoint. Including the n value gave a better correlation than excluding it. Our interpretation was that this supplemental information is needed since the tendencies of μ_B and τ_y are too similar in the lower DI_{30} range for some hematocrit level to determine the unique set of DI_{30} and μ_p. The outputs of this network are plasma viscosity μ_p and the deformability DI_{30}. This network, shown in Figure 8, contains 9 units in a hidden layer. In the figure, I(1), I(2), I(3), I(4), O(1), and O(2) are the normalized input and output parameter values of μ_B, τ_y, n, hematocrit, μ_p, and DI_{30}, respectively. The range of those values, normalized by Eq. 4, are 0.1 to 0.9:

$$X' = \frac{X - X_{min}}{1.25(X_{max} - X_{min})} + 0.1, \tag{4}$$

where X and X' are the measured and normalized parameter values, while X_{max} and X_{min} are the maximum and minimum measured parameter values for each parameter listed in Table 1. The inverse of Eq. 4 makes the predicted parameter values from the output $O(k)$. Equation 5 shows the relation between the inputs and outputs of the network:

$$O(k) = \sum_{j=1}^{9} \left[\frac{W_2(k,j)}{1 + \exp\left\{ -\left(\sum_{i=1}^{4} W_1(j,i) I(i) \right) - B_1(j) \right\}} \right] + B_2(k). \tag{5}$$

Table 2. Coefficient Values of $W_1(j, i)$

	$i=1$	2	3	4
$j=1$	0.56	−6.00	0.95	−1.56
2	−3.94	1.39	2.31	−1.61
3	0.37	1.65	−0.45	0.67
4	−1.43	−3.57	−0.11	0.53
5	2.55	1.86	−1.64	−3.26
6	0.22	−0.53	−1.34	0.65
7	−1.02	1.21	−1.78	−0.67
8	−0.46	−3.15	0.43	−3.62
9	−4.54	2.64	2.26	−1.90

Table 3. Coefficient Values of $W_2^T(k, j)$

	$k=1$	2
$j=1$	0.50	5.12
2	−2.40	−2.12
3	−1.86	−0.61
4	1.56	2.55
5	2.76	−0.52
6	0.73	1.37
7	−2.08	1.36
8	2.73	2.59
9	−3.09	−3.29

Table 4. Coefficient Values of $B_1(j)$ and $B_2(k)$

	$B_1(j)$		$B_2(k)$
$j=1$	−1.10	$k=1$	0.29
2	0.28	2	−0.24
3	0.04		
4	1.33		
5	1.90		
6	0.90		
7	0.08		
8	1.86		
9	−0.42		

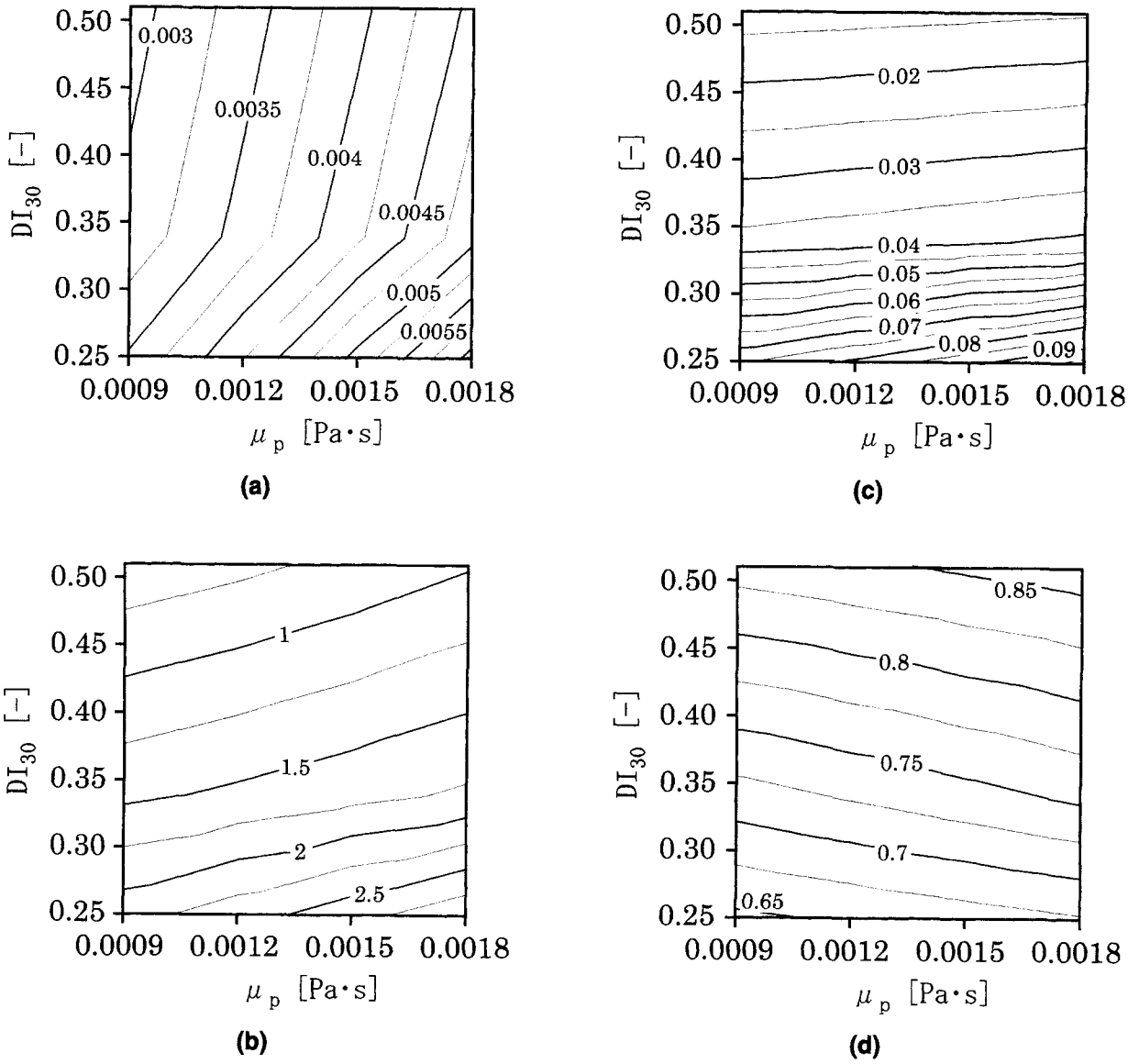

Figure 6. Contour maps on μ_p–DI plane of (a) μ_B, (b) τ_y, (c) k, and (d) n (Hct = 47).

Optimization of coefficients W and B in Eq. 5 gives the correlation function of this relation. This optimization process is called leaning, and the so-called backpropagation method was employed. MATLAB performed all the processing in this study. The coefficients obtained are shown in Tables 1–4, as are the values used for normalization in Eq. 4. It is not difficult to utilize the network as an empirical formula by using the values in the lists, and so the authors could distribute its BASIC program by e-mail for the convenience of other researchers.

Correlation accuracy

Figure 9 shows the correlation accuracy after enough learning. Horizontal and vertical axes represent the measured and the predicted values, respectively. Broken lines in the figure show the range plus/minus the 10% relative error. It can be seen that both indices could be correlated accurately enough by means of an introduced feedforward artificial neural network. After reference to the coefficients listed in the tables, it is concluded that the equation presented in this study can be utilized as an empirical formula. Further, it should be noted here that the authors confirmed the inaccuracy of the linear correlation.

Validation of the proposed method

For the purpose of validation, the new estimation method was applied to 20 whole-blood samples collected from the personnel working in the hospital and some of the authors. Figure 10 shows the comparison between the measured plasma viscosity and predicted values by the network. It can be seen that the predicted values are somewhat higher, but almost in the normal range. Figure 11 shows the relation between the hematocrit and predicted DI_{30}. As shown in the figure, the DI_{30} values are also slightly higher than the nor-

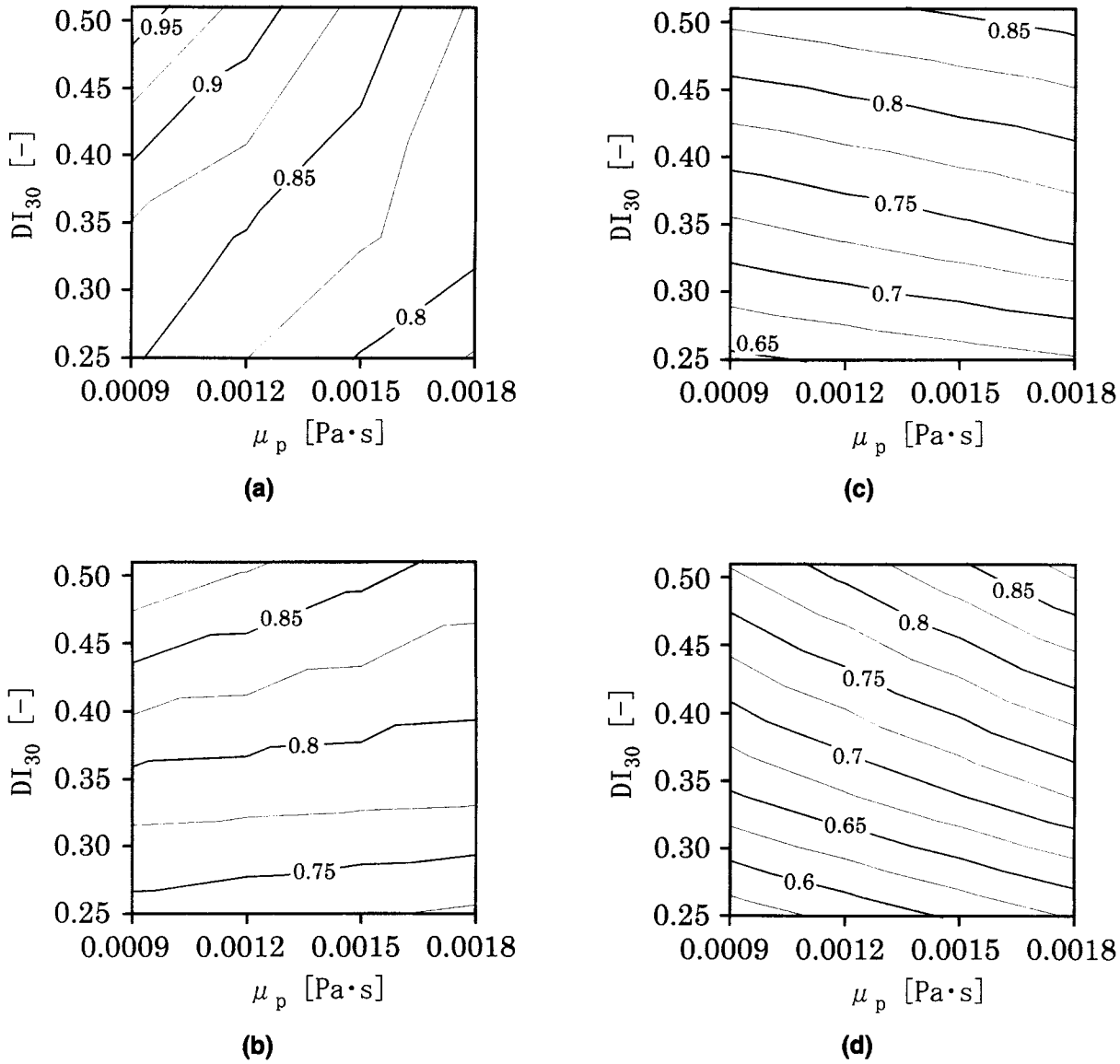

Figure 7. Change of contour map of *n* with increase of hematocrit: (a) Hct = 27; (b) Hct = 37; (c) Hct = 47; (d) Hct = 57.

mal value shown by the line, which is the value of the untreated red cells. Although the DI_{30} values of those samples were not available, they distribute sharply in the normal range even though the hematocrit values vary widely in the physiologically normal range. Therefore, it is expected from these figures that the proposed method can be practically applicable to clinical usage.

Discussion

Although both of the predicted values are relatively high, this seems to be because of the difficulty in keeping blood fresh for the experiments. Therefore, there is a possibility that the properties of plasma and red cells are somewhat different from the fresh samples in spite of the usage of anticoagulant. This problem could not be avoided since all test fluids were prepared from the blood samples collected from only

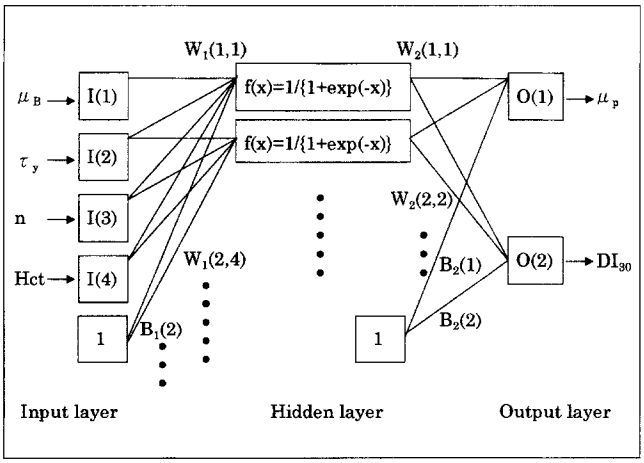

Figure 8. Feedforward neural network.

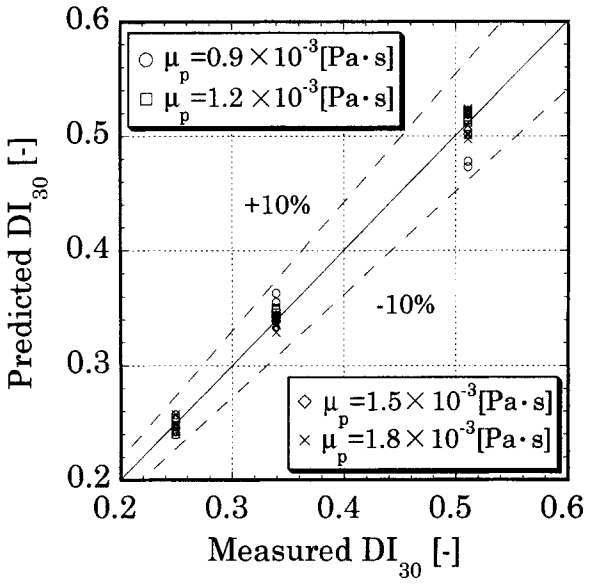

(a)

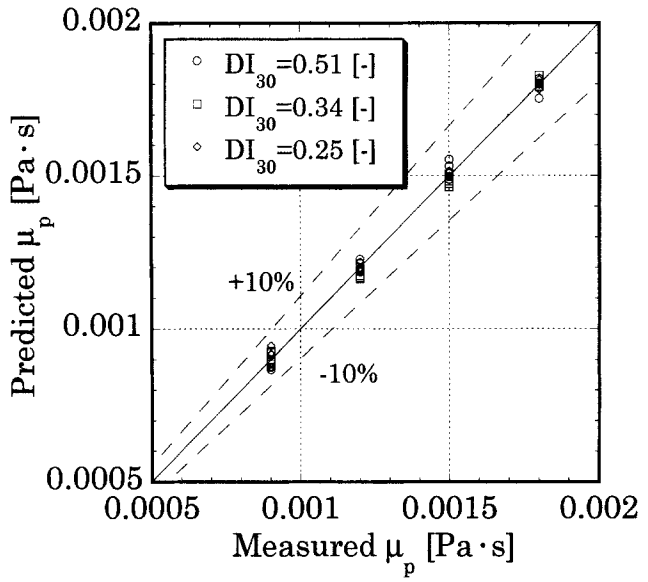

(b)

Figure 9. Correlation accuracy after enough learning for (a) DI_{30} and (b) μ_p.

two donors. Instead, however, it should be noted that this fact made it possible to investigate the interactive influence of each factor, that is, the red-cell deformability, hematocrit, and plasma viscosity, while independently excluding other factors as much as possible. Further, the authors argue that the appropriate arrangement of discrete data is absolutely indispensable for obtaining a correlation function that is widely valid. Fine-tuning of the present neural network based on the data obtained using fresh samples is the work pursued in the future.

Since there are several definitions for the red-cell deformability, and different factors result in the same range of

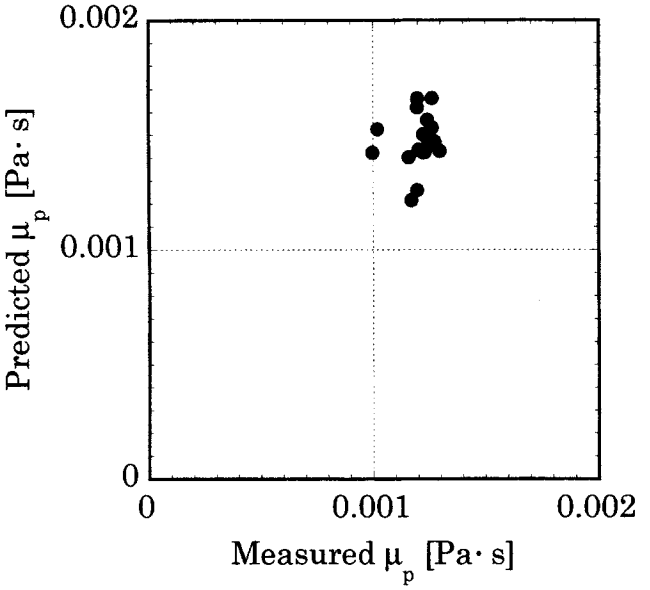

Figure 10. Comparison between measured and predicted μ_p.

decreased deformability by a different mechanism, the proposed DI_{30} cannot be unique for all clinical purposes. Another definition might be preferable for a specific disease. The authors believe that the frame of this work can be applicable to other definitions, namely, another index for the deformability can be substituted for the DI_{30} used in this study. Further investigation will be needed to extend this study to other definitions and to utilize this method as a test for a particular disease.

Conclusion

A new estimation method of clinical blood indices such as red-cell deformability and plasma viscosity is proposed in this

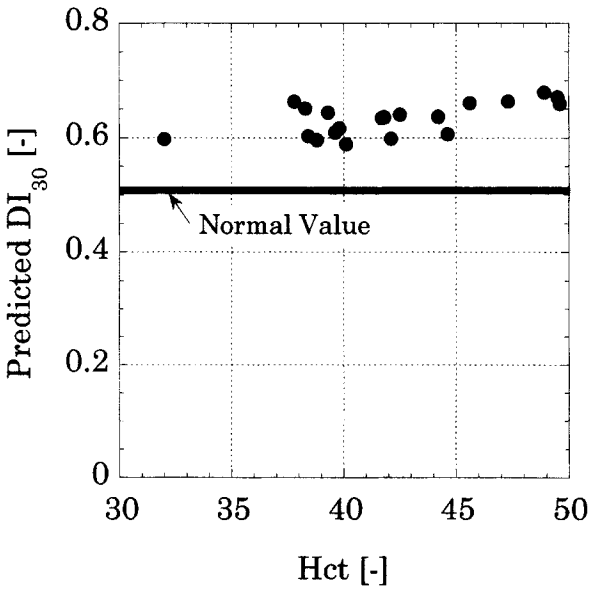

Figure 11. Predicted DI_{30} and hematocrit.

study. This method is based on the relation between the flow-characteristics parameters and the clinical indices that were obtained by comprehensive experiments. Bingham and power law models were adopted as non-Newtonian models to extract the features of the flow curves efficiently. A feedforward artificial neural network is utilized to predict the red-cell deformability and plasma viscosity from hematocrit, Bingham viscosity μ_B, yield stress τ_y, and fluid behavior index n. It was confirmed that the network gave good agreement with measured values. Further, this method was applied to 20 healthy people. It was concluded that this method was practically applicable to clinical usage, since the predicted values were in a reasonable range. By performing more detailed experiments on fresh blood and fine-tuning the coefficients of the network based on the present work, the accuracy is expected to be improved in the future.

Acknowledgment

We thank donors who are persons working at Gunma Prefectural Cardiovascular Center, Mr. Okatsu, and Mr. Wakatsuki. The advice of Dr. Kuroda and Dr. Yoshikawa is fully acknowledged.

Literature Cited

Bessis, M., and N. Mohandas, "A Diffractometric Method for the Measurement of Cellular Deformability," *Blood Cells*, **1**, 307 (1975).

Chien, S., "Principles and Techniques for Assessing Erythrocyte Deformability," *Red Cell Rheology*, M. Bessis, S. B. Shohet, and N. Mohandas, eds., Springer-Verlag, Berlin, p. 71 (1978).

Clark, M. R., N. Mohandas, and S. R. Shohet, "Deformability of Oxygenated Irreversibly Sickled Cells," *J. Clin. Invest.*, **65**, 189 (1980).

Demath, H., and M. Beale, *Neural Network Toolbox User's Guide*, The Math Works Inc., unpublished (1994).

Evans, E. A., and P. L. La Celle, "Intrinsic Material Properties of the Erythrocyte Membrane Indicated by Mechanical Analysis of Deformation," *Blood*, **45**, 29 (1975).

Evans, E., N. Mohandas, and A. Leung, "Static and Dynamic Rigidities of Normal and Sickle Erythrocytes, Major Influences of Cell Homoglobin Concentration," *J. Clin. Invest.*, **73**, 477 (1984).

Green, M. A., C. T. Noguchi, A. J. Keidan, S. S. Marwah, and J. Stuart, "Polymerization of Sickle Cell Hemoglobin at Arterial Oxygen Saturation Impairs Erythrocyte Deformability," *J. Clin. Invest.*, **81**, 1669 (1988).

Ham, T. H., R. W. Sayre, R. F. Dunn, and J. R. Murohy, "Physical Properties of Red Cells as Related to Effects in Vivo. II. Effect of Thermal Treatment on Rigidity of Red Cells, Stroma and the Sickle Cell," *Blood*, **32**, 862 (1968).

Ikemoto, S., T. Maeda, H. Tanaka, T. Yokose, J. Yamamoto, S. Kawakami, Y. Isogai, K. Kanai, K. Inami, and I. Ohtani, "Analysis of Red Blood Cell Deformability with a New Type Apparatus, DF-1," *Proc. Jikei Symp. on Hemorheology*, Y. Isogai, ed., Medical Review Company, Tokyo, p. 43 (1998).

Ikemoto, S., H. Tanaka, J. Yamamoto, K. Kuchiba, M. Akiyama, T. Maeda, T. Yokose, and Y. Isogai, "Abnormal Red Cell Deformability in Iron Deficiency Anemia," *Jikeikai Med. J.*, **36**, 363 (1989).

Keidan, A. J., C. T. Noguchi, M. Player, S. M. Chalder, and J. Stuart, "Erythrocyte Heterogeneity in Sickle Cell Disease: Effect of Deoxgenation on Intracellular Polymer Formation and Rheology of Sub-populations," *Br. J. Haematol.*, **72**, 254 (1989).

Maeda, T., J. Ogawa, K. Kuchiba, M. Akiyama, S. Ikemoto, T. Yokose, and Y. Isogai, "Determinants of Red Cell Deformability in Diabetics," *Proc. Int. Symp. on Treatment of Diabetes Mellitus*, N. Sakamoto, K. G. M. M. Alberti, and N. Hotta, eds., Elsevier, Nagoya, p. 383 (1990).

Mohandas, N., and J. A. Chasis, "Red Blood Cell Deformability, Membrane Material Properties and Shape: Regulation by Transmembrane, Skeletal and Cytosolic Proteins and Lipids," *Semin. Hematol.*, **30**, 171 (1993).

Nagasawa, T., "Deformation of Transforming Red Cells in Various pH Solutions," *Experientia*, **37**, 977 (1981).

Nagasawa, T., "Red Cell Deformability Measured by Laser Diffractometry," *Recent Advances in Hemorheology*, Y. Isogai, ed., Medical Review Company, Tokyo, p. 146 (1992).

Ogawa, K., S. Ookawara, S. Ito, K. Taniguchi, and M. Doi, "Blood Viscometer with Vacuum Glass Suction Tube and Needle," *J. Chem. Eng. Jpn.*, **24**, 215 (1991).

Ogawa, K., S. Ookawara, and K. Taniguchi, "Non-Newtonian Flow Characteristics of Blood in the Shear Rate Range of 100–10,000 s^{-1}," *J. Chem. Eng. Jpn.*, **27**, 610 (1994).

Schmalzer, E. A., R. S. Manning, and S. Chien, "Filtration of Sickle Cells: Recruitment into a Rigid Fraction as a Function of a Density and Oxygen Tension," *J. Lab. Clin. Med.*, **113**, 727 (1989).

Schmid-Schönbein, H., and R. Wells, "Fluid Drop-Like Transition of Erythrocytes Under Shear," *Science*, **165**, 288 (1969).

Usami, S., S. Chien, and J. F. Bertles, "Deformability of Sickle Cells as Studied by Microsieving," *J. Lab. Clin. Med.*, **86**, 274 (1975).

Yip, R., N. Mohandas, M. R. Clark, S. Jain, S. B. Shohet, and P. R. Dallman, "Red Cell Membrane Stiffness in Iron Deficiency," *Blood*, **62**, 99 (1983).

Manuscript received Sept. 14, 1999, and revision received June 23, 2000.